Hect E3 ubiquitin ligase Tom1 controls Dia2 degradation during the cell cycle

Dong-Hwan Kim and Deanna M. Koepp
Department of Genetics, Cell Biology and Development, University of Minnesota, Minneapolis, MN 55455

ABSTRACT **The ubiquitin proteasome system plays a pivotal role in controlling the cell cycle. The budding yeast F-box protein Dia2 is required for genomic stability and is targeted for ubiquitin-dependent degradation in a cell cycle–dependent manner, but the identity of the ubiquitination pathway is unknown. We demonstrate that the Hect domain E3 ubiquitin ligase Tom1 is required for Dia2 protein degradation. Deletion of *DIA2* partially suppresses the temperature-sensitive phenotype of *tom1* mutants. Tom1 is required for Dia2 ubiquitination and degradation during G1 and G2/M phases of the cell cycle, whereas the Dia2 protein is stabilized during S phase. We find that Tom1 binding to Dia2 is enhanced in G1 and reduced in S phase, suggesting a mechanism for this proteolytic switch. Tom1 recognizes specific, positively charged residues in a Dia2 degradation/NLS domain. Loss of these residues blocks Tom1-mediated turnover of Dia2 and causes a delay in G1–to–S phase progression. Deletion of *DIA2* rescues a delay in the G1–to–S phase transition in the *tom1*Δ mutant. Together our results suggest that Tom1 targets Dia2 for degradation during the cell cycle by recognizing positively charged residues in the Dia2 degradation/NLS domain and that Dia2 protein degradation contributes to G1–to–S phase progression.**

Monitoring Editor
Mark J. Solomon
Yale University

Received: Jul 25, 2012
Revised: Aug 20, 2012
Accepted: Aug 24, 2012

INTRODUCTION

The highly conserved ubiquitin proteasome system (UPS) plays a role in a number of cellular processes, including cell cycle control, DNA replication, and DNA damage response (Nakayama and Nakayama, 2006; Kouranti and Peyroche, 2012; Silverman *et al.*, 2012). In budding yeast, the F-box protein Dia2 serves as an adaptor for a multicomponent Skp1/Cdc53/F-box protein (SCF) E3 ubiquitin ligase complex and functions to maintain genomic stability (Blake *et al.*, 2006; Koepp *et al.*, 2006; Pan *et al.*, 2006). Dia2 assembles with the components of the replisome complex and regulates the progression of the DNA replication fork (Mimura *et al.*, 2009; Morohashi *et al.*, 2009), suggesting a role in controlling S-phase progression.

Dia2 itself is an unstable protein targeted for degradation by the UPS (Mimura *et al.*, 2009; Kile and Koepp, 2010). There are conflicting reports about the pathway responsible for Dia2 protein turnover. One study suggests that Dia2 degradation is the result of an autoubiquitination pathway (Mimura *et al.*, 2009), similar to other F-box proteins (Zhou and Howley, 1998; Kus *et al.*, 2004). By contrast, our previous work indicates that an SCF-independent pathway targets Dia2 for degradation, as deletion of the F-box domain required for binding the core SCF complex does not stabilize the protein. Rather, a 20–amino acid motif that overlaps with a nuclear localization sequence (NLS)-containing domain was found to be required for Dia2 protein turnover (Kile and Koepp, 2010). However, the identity of the ubiquitin ligase responsible for targeting Dia2 for degradation via this domain was not determined.

The Dia2 protein turnover rate varies throughout the cell cycle. Dia2 is at its most unstable during G1 phase, is moderately unstable during G2/M, and is substantially stabilized in S phase. Dia2 protein stabilization is dependent on the activation of the S-phase checkpoint pathway (Kile and Koepp, 2010). One model that explains these observations is that Dia2 is stabilized after checkpoint activation so that the SCF^{Dia2} complex may assemble to target S phase–specific proteins for degradation. Two identified targets include replication proteins Mrc1 and Ctf4, although no physiological role

This article was published online ahead of print in MBoC in Press (http://www.molbiolcell.org/cgi/doi/10.1091/mbc.E12-07-0548) on August 29, 2012.

Address correspondence to: Deanna M. Koepp (koepp015@umn.edu).

Abbreviations used: αF, alpha factor; GST, glutathione *S*-transferase; HU, hydroxyurea; NLS, nuclear localization sequence; RT-PCR, reverse transcription PCR; SCF, Skp1/Cdc53/F-box protein; UPS, ubiquitin proteasome system.

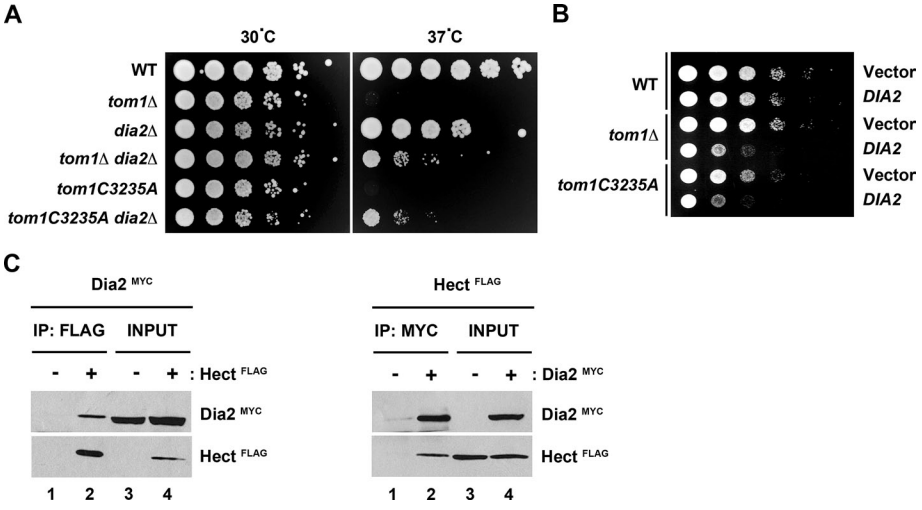

FIGURE 1: Tom1 genetically and physically interacts with Dia2. (A) The temperature-sensitive phenotype of *tom1*Δ and *tom1C3235A* mutants is partially suppressed by deletion of *DIA2*. The indicated strains were grown to mid–log phase and spotted in 10-fold serial dilutions onto rich medium plates. The plates were incubated at 30°C and 37°C for 2 d. (B) Overexpression of *DIA2* results in a growth defect in *tom1*Δ and *tom1C3235A* mutants. The 10-fold serial dilutions of wild-type, *tom1*Δ, and *tom1C3235A* cells carrying empty vector or *DIA2* under the control of *GAL1,10* promoter were spotted onto minimal plates with 2% galactose. Plates were incubated at 30°C for 2–3 d. (C) The Hect domain of Tom1 binds to Dia2. Hi5 insect cells were coinfected with Flag-Tom1 Hect domain and Myc-Dia2 baculoviruses. Flag-Tom1 Hect domain or Myc-Dia2 protein was immunoprecipitated with anti-Flag or anti-Myc antibodies and analyzed by immunoblotting. (–) and (+) represent uninfected and infected with the indicated baculoviruses. Anti-Flag or anti-Myc antibodies were added to the indicated immunoprecipitation assays.

for their degradation has yet been established (Mimura *et al.*, 2009).

In this article. we identify the E3 ubiquitin ligase that targets Dia2 for ubiquitin-mediated degradation and describe how Dia2 is recruited to the degradation pathway. Moreover, we show that failure to degrade Dia2 leads to a cell cycle progression defect.

RESULTS

Tom1 targets Dia2 for ubiquitin-dependent degradation

To identify the E3 ubiquitin ligase that targets Dia2 for degradation, we carried out a candidate approach. Based on the literature, the Hect domain E3 ubiquitin ligase Tom1 was a promising candidate, as it has been shown to interact with Yra1 (Iglesias *et al.*, 2010), a protein required for Dia2 association with chromatin (Swaminathan *et al.*, 2007), and Rad53, an S-phase checkpoint kinase (Iglesias *et al.*, 2010). We first asked whether there was a genetic relationship between Tom1 and Dia2 by examining the growth of wild-type, *tom1*Δ, *dia2*Δ, and *tom1*Δ *dia2*Δ strains at 30°C and 37°C. Interestingly, the temperature-sensitive phenotype of the *tom1*Δ mutant was partially suppressed by deletion of *DIA2* at 37°C (Figure 1A). The *dia2*Δ mutant also partially rescued the temperature-sensitive phenotype of the *tom1C3235A* mutant in which the catalytic cysteine is replaced with alanine. These results suggest the temperature-sensitive phenotype of *tom1*Δ and *tom1C3235A* mutants may be due in part to aberrant accumulation of the Dia2 protein. If this were the case, we would expect that overexpression of *DIA2* in *tom1*Δ cells would also lead to a growth defect more significant than the mild defect observed when *DIA2* is overexpressed in wild-type cells. To test this, we overexpressed *DIA2* in wild-type, *tom1*Δ, and *tom1C3235A* mutants using the *GAL1,10* galactose-inducible promoter. Under these conditions, overexpression of *DIA2* caused a stronger growth defect in *tom1*Δ and *tom1C3235A* mutants than in wild-type cells (Figure 1B).

To determine whether Tom1 and Dia2 physically interact, we performed an in vitro binding assay using the Flag-tagged Hect domain of Tom1 and Myc-tagged Dia2 expressed from insect cells. When the Flag-tagged Hect domain of Tom1 was purified, Myc-tagged Dia2 coprecipitated. Reciprocal copurification of the Flag-tagged Hect domain of Tom1 was observed when Myc-tagged Dia2 was immunoprecipitated (Figure 1C).

The most straightforward explanation for these results is that Tom1 targets Dia2 for ubiquitin-dependent degradation. To explore whether Tom1 is required for Dia2 protein degradation, we first assessed the turnover of the Dia2 protein in *tom1* mutants, using a cycloheximide stability assay. Wild-type, *tom1*Δ, and *tom1C3235A* cells were grown to mid–log phase, and Dia2 protein abundance was measured over time. We observed that Dia2 was partially stabilized in both *tom1*Δ and *tom1C3235A* mutants compared with wild-type (Figure 2A). Notably, Dia2 mRNA abundance was not changed in the *tom1*Δ mutant (Figure 2B), indicating that the change in Dia2 protein levels was not the result of transcriptional regulation. To examine Dia2 ubiquitination, we developed an in vitro ubiquitination assay using fractionated yeast extracts and glutathione *S*-transferase (GST)-Dia2 purified from insect cells. When extracts from wild-type cells were incubated with GST-Dia2 in the presence of E1, an ATP regeneration system, and ubiquitin, Dia2 ubiquitin conjugates were observed (Figure 2C, lane 3). However, Dia2 ubiquitin conjugates were significantly reduced when extracts from the *tom1*Δ strain were used (Figure 2C, lane 5), indicating that Dia2 ubiquitination is dependent on Tom1. Together our results suggest that Tom1 targets Dia2 for ubiquitin-mediated degradation.

Tom1 controls Dia2 proteolysis during G1 and G2/M

Dia2 is unstable during G1 and G2/M phases of the cell cycle but is stabilized during S phase or in response to activation of the S-phase checkpoint (Kile and Koepp, 2010). We investigated when during the cell cycle Tom1 controls Dia2 turnover by performing stability assays in cells synchronized in G1 by alpha factor (αF) and in early S phase by hydroxyurea (HU), which also activates the S-phase checkpoint, or at metaphase with nocodazole. As shown in Figure 3A, Dia2 was turned over in wild-type but stabilized in *tom1*Δ and *tom1C3235A* mutants in G1. In contrast, no significant turnover of Dia2 was observed in *tom1*Δ and *tom1C3235A* mutants in cells arrested with HU (Figure 3B). However, we found that Dia2 was partially stabilized in *tom1*Δ and *tom1C3235A* mutants in cells arrested by nocodazole (Figure 3C), suggesting that Tom1 is required for Dia2 proteolysis during G2/M. We conclude that degradation of Dia2 during G1 and G2/M phases of the cell cycle is dependent on Tom1.

The mechanistic basis for how Dia2 is stabilized in response to initiation of S phase or S-phase checkpoint activation is not known. With the identification of Tom1 as the E3 ubiquitin ligase

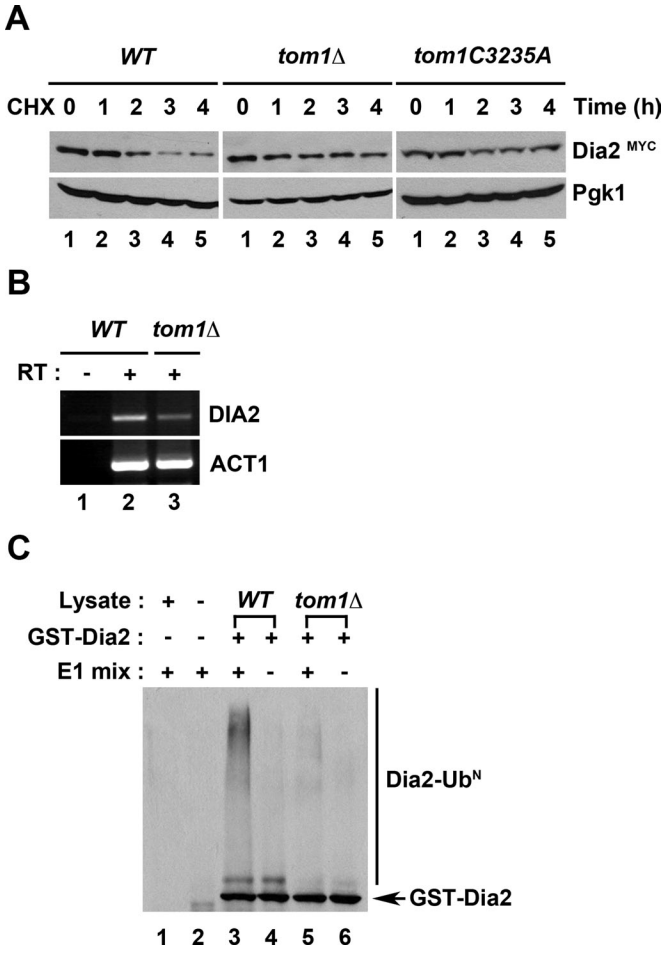

FIGURE 2: Tom1 is required for ubiquitin-dependent Dia2 degradation. (A) Dia2 is partially stabilized in *tom1*Δ and *tom1C3235A* mutants. Wild-type, *tom1*Δ, and *tom1C3235A* cells were grown to mid–log phase and treated with cycloheximide (100 µg/ml). Samples were taken at the indicated times and processed for stability assay. Immunoblotting was performed with anti-Myc and anti-Pgk1 antibodies. Pgk1 was used as a loading control. (B) Dia2 mRNA levels are not changed in the *tom1*Δ mutant. RT-PCR was conducted to examine the level of Dia2 transcript in wild-type and *tom1*Δ strains. *ACT1* was used as a loading control. RT, reverse transcriptase. (C) In vitro ubiquitination of Dia2. GST-Dia2 protein expressed from baculovirus-infected insect cells was purified using glutathione-Sepharose 4B beads. GST-Dia2 protein was incubated with ubiquitin, E1, ATP, an ATP regeneration system, and fractionated yeast extracts purified from wild-type or *tom1*Δ strains at 30°C for 45 min. Samples were run on 6% SDS–PAGE and immunoblotted with anti-GST antibodies.

that targets Dia2 for degradation, one possible explanation is that Tom1 and Dia2 no longer interact during S phase or in response to S-phase checkpoint activation. To test this idea, we conducted coimmunoprecipitation assays in synchronized cells (Figure 3D). Cells expressing Myc-tagged Dia2 and Flag-tagged Tom1 from their endogenous loci were arrested in late G1 with αF, in early S phase with HU, and in G2/M phase with nocodazole. When Flag-tagged Tom1 was immunoprecipitated from αF-arrested cells, we observed significant coprecipitation of Myc-tagged Dia2. However, this coprecipitation was almost completely absent in HU-arrested cells. In contrast, we observed a modest interaction between Tom1 and Dia2 in nocodazole-arrested cells. Thus inhibition of the interaction between Tom1 and Dia2 may explain the proteolytic switch observed as cells enter S phase or when the S-phase checkpoint is activated.

Tom1 recognizes a stretch of positively charged residues in Dia2

We have previously shown that a domain just upstream of the F-box in Dia2, which also contains two canonical NLSs, was required for Dia2 protein turnover. Although nuclear localization is required for Dia2 degradation, this domain is also likely important for recognition by the degradation pathway, as the addition of an exogenous NLS to a Dia2 mutant lacking this domain is still stabilized (Kile and Koepp, 2010). We hypothesized that Tom1 may bind to this domain in Dia2, so we tested whether various truncated Dia2 mutants are able to coimmunoprecipitate Tom1 (Figure 4). We generated strains expressing epitope-tagged Tom1 and the Dia2 mutants expressed from their endogenous loci (Figure 4, top, left panel). As shown in Figure 4, Tom1 and full-length Dia2 coimmunoprecipitate. The Dia2 mutants used include a mutant containing only the N-terminal tetratricopeptide repeat (*TPR*), a mutant in which the F-box domain was deleted in frame (Δ*F-box*), a mutant that lacks the first 149 amino acids of the N-terminus (Δ*N149*), and a mutant with the NLS/degradation domain deleted in frame but containing an exogenous SV40 large T antigen (Tag) NLS attached to the N-terminus (SVΔNLS). In the coimmunoprecipitation assay, all Dia2 proteins, except the SVΔNLS mutant, copurify with Tom1, although the binding of the ΔF-box and TPR proteins may be somewhat reduced relative to wild-type Dia2. These results suggest that the NLS domain of Dia2 is required for its interaction with Tom1.

The domain in Dia2 required for degradation consists of two stretches of lysine residues interrupted by a nine-residue sequence. Our coimmunoprecipitation results were unable to determine which sections of this domain were required for recruitment to Tom1. We speculated that there were three possibilities: 1) Tom1 may recognize the lysine residues, perhaps even use them as sites of ubiquitin conjugation; 2) Tom1 may recognize the nine-residue sequence in between the lysines; or 3) Tom1 recognizes positively charged residues. To distinguish among these possibilities, we generated three mutants, one in which the lysines were changed to arginines to conserve charge (Dia2-KR), one in which the lysines were mutated to alanines (Dia2-KA), and one in which the nine-residue middle sequence was deleted in frame (Dia2Δ185-193; Figure 5A). For the Dia2-KA and Dia2Δ185-193 proteins, we also added the SV40 Tag NLS to the N-terminus to avoid altering the nuclear localization of Dia2 (SVDia2-KA, SVDia2Δ185-193). We used a full-length Dia2 with the SV40 Tag NLS fused to the N-terminus (SVDia2) as a control for these mutants. We examined the stability of these proteins using the cycloheximide stability assay in G1-arrested cells. As shown in Figure 5B, the turnover rates of wild-type Dia2 and the Dia2-KR mutant were indistinguishable, indicating that exchanging the lysines with arginines has no effect on Dia2 protein turnover. Intriguingly, the SVDia2-KA mutant protein was significantly stabilized in αF-arrested cells, whereas both the SVDia2 and SVDia2Δ185-193 proteins were turned over with similar rates (Figure 5C). These results indicate that it is not the lysine residues per se, but rather the positive charge of these residues in the Dia2 degradation domain that are necessary for protein turnover.

On the basis of the stability assay results, we predicted that the positively charged residues in the NLS/degradation domain would be required for Tom1 to bind Dia2. To test this, we carried out a coimmunoprecipitation assay using strains expressing epitope-tagged Dia2-KR or SVDia2-KA proteins and Flag-tagged Tom1.

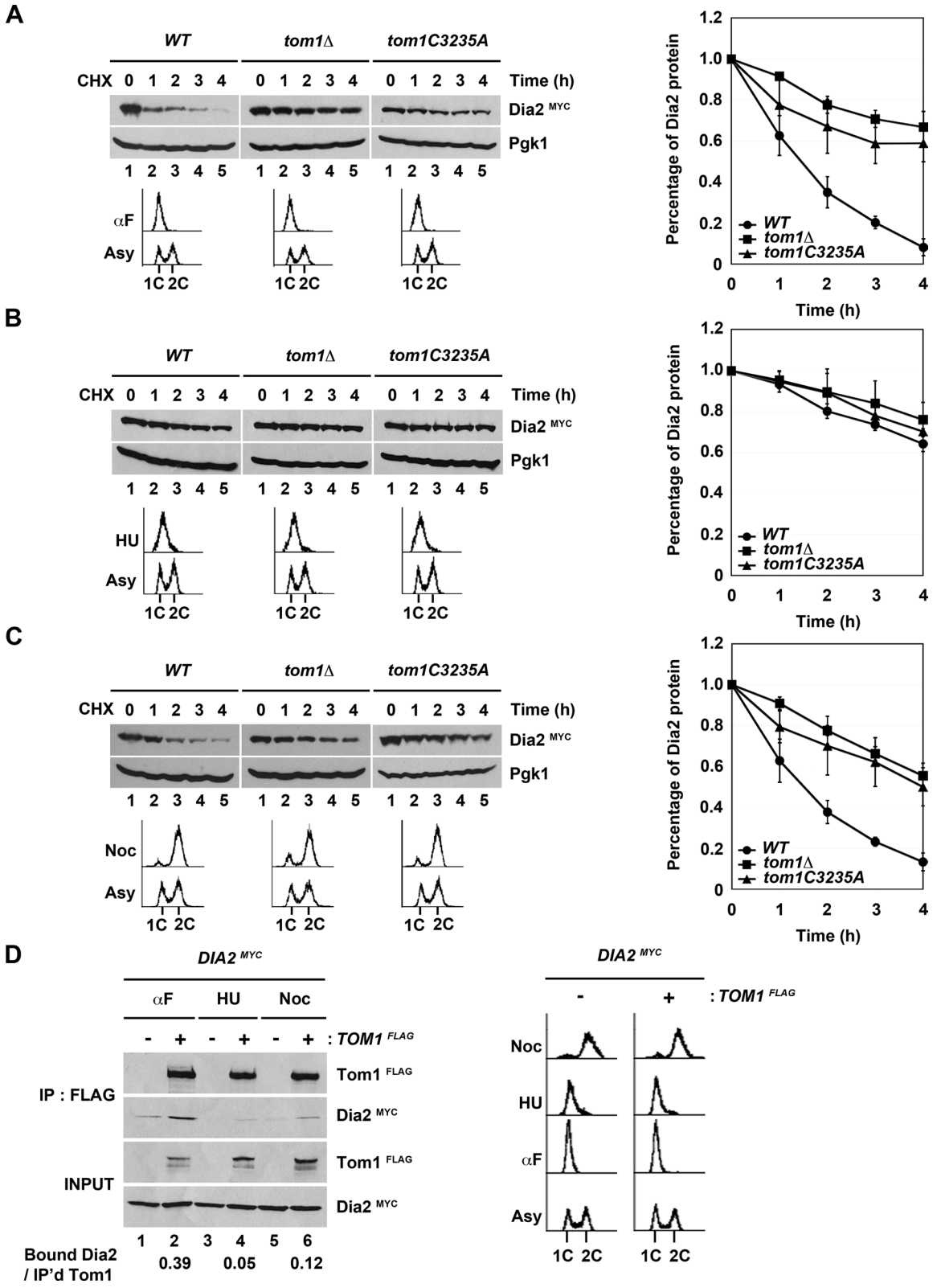

FIGURE 3: Tom1 regulates Dia2 turnover in G1 and G2/M. (A) Dia2 stabilization in *tom1Δ* and *tom1C3235A* mutants in G1 phase. Wild-type, *tom1Δ*, and *tom1C3235A* strains were arrested with αF for 3 h. After cycloheximide treatment (100 μg/ml), samples were collected at the indicated times and immunoblotted with anti-Myc antibodies. Pgk1 was used as a loading control. Flow cytometry analysis was performed to monitor the αF arrest. Dia2 protein turnover was quantified with three independent experiments. Error bars indicate SDs. (B) Dia2 is stable in S phase. The indicated strains were arrested with 200 mM HU for 3 h. Samples were taken at the indicated times after cycloheximide treatment (100 μg/ml) and analyzed by immunoblotting with anti-Myc antibodies. Pgk1 was used as a loading control. Three independent results were used to quantify the rate of Dia2 turnover. Error bars indicate standard deviations. The HU

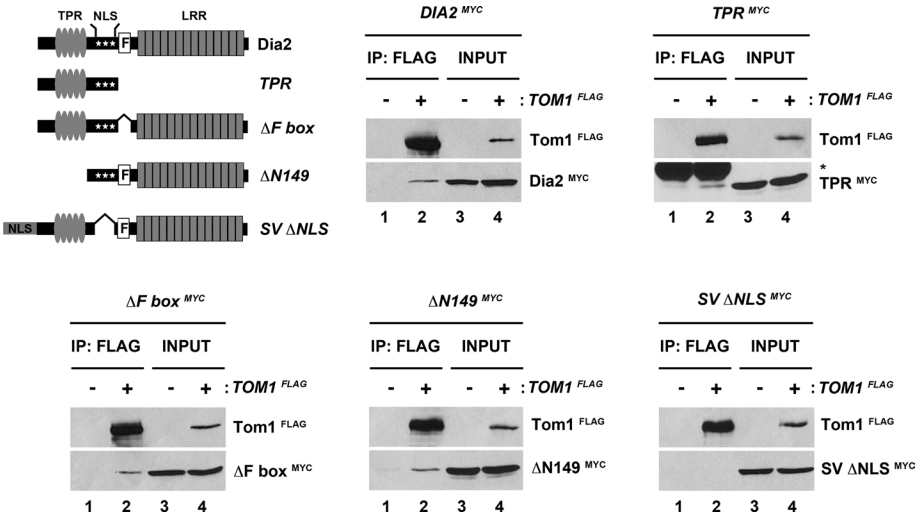

FIGURE 4: Tom1 binds to Dia2 through the degradation/NLS domain of Dia2. Endogenously expressed Tom1 and Dia2 coprecipitate each other via the degradation/NLS domain of Dia2. The indicated strains were grown to mid–log phase. Total cell lysates (2 mg) were immunoprecipitated with anti-Flag antibodies and immunoblotted with anti-Flag and anti-Myc antibodies.

We observed that Flag-tagged Tom1 coprecipitated with Dia2-KR but not with the SVDia2-KA protein (Figure 5D). Together these results suggest that Tom1 specifically recognizes the positive charge on the lysine residues in the Dia2 NLS/degradation domain.

Defects in Dia2 protein turnover lead to a G1–to–S phase progression delay

If degradation of Dia2 via Tom1 is the major pathway for Dia2 degradation, we would expect that overexpression of a Dia2 mutant unable to bind Tom1 would produce a stronger overexpression phenotype than full-length Dia2 in wild-type cells. Also, if Tom1 recognizes only the positively charged residues in the Dia2 degradation/NLS domain, we would also expect that overexpression of the *SVdia2-KA* mutant would be indistinguishable from the *DIA2* overexpression phenotype in *tom1*Δ cells. To test these predictions, we examined the overexpression phenotypes of full-length *DIA2*, *dia2-KR*, *SVdia2-KA*, and *SVdia2-*Δ*185-193* mutants in wild-type and *tom1*Δ cells (Figure 6A). We observed that both wild-type and *tom1*Δ cells overexpressing the *dia2-KR* mutant behaved as the parental strains overexpressing full-length *DIA2*. By contrast, overexpression of the *SVdia2-KA* mutant impaired the growth of wild-type cells compared with cells overexpressing full-length *SVDIA2* or *SVdia2-*Δ*185-193*. Moreover, the growth defect of *tom1*Δ cells caused by *DIA2* overexpression was indistinguishable from overexpression of the *SVdia2-KA* mutant and looked similar to the results seen when *SVdia2-*Δ*185-193* is overexpressed (Figure 6A). These results suggest that Tom1 is the primary E3 ubiquitin ligase that controls Dia2 protein turnover, recognizing specific, positively charged residues in the degradation/NLS domain.

We have previously reported that the stabilized forms of *dia2* mutants, such as *SV*Δ*214* and *SV*Δ*NLS*, modestly increased the percentage of G1 cells in an asynchronous population (Kile and Koepp, 2010). Therefore we would expect a similar phenotype to be observed in the *SVdia2-KA* mutant. To test this, wild-type cells carrying overexpression constructs for *SVDIA2* or *SVdia2-KA* were grown to mid–log phase and their cell cycle distributions were measured by flow cytometry (Figure 6B). Consistent with previous results, overexpression of *SVDIA2* showed a modest increase in G1 cells relative to cells carrying an empty vector. Furthermore, cells expressing *SVdia2-KA* exhibited a significant increase in the G1 population. These results suggest that the *dia2-KA* mutant may transit more slowly through G1 phase into S phase than wild-type cells (Figure 6B). To test this possibility, we arrested the same strains with αF, released them into medium containing nocodazole, and monitored cell cycle progression from late G1 to metaphase (Figure 6B). Cells overexpressing the *SVDIA2* exhibited a mild delay in the G1–to–S phase transition compared with the control cells. In addition, overexpression of the *SVdia2-KA* mutant prolonged the delay in G1–to–S phase progression (Figure 6B), suggesting that Dia2 protein turnover is important for a proper progression from G1 to S phase. We then asked whether the *tom1*Δ mutant also exhibits the same delay in the G1–to–S phase transition, as would be expected if Dia2 is a significant target of Tom1. Wild-type, *tom1*Δ, *dia2*Δ, and *tom1*Δ *dia2*Δ strains arrested with αF were released into rich medium containing nocodazole, and cell cycle progression from late G1 to metaphase was monitored (Figure 6C). Under these conditions, the *tom1*Δ mutant proceeded into S phase from G1 phase with a 5-min delay, compared with wild-type and the *dia2*Δ mutant. Interestingly, the delay in G1–to–S phase progression observed in the *tom1*Δ mutant was rescued by deletion of *DIA2* (Figure 6C). These findings indicate that Tom1-mediated Dia2 turnover in G1 is required for an efficient G1–to–S phase transition.

DISCUSSION

Our results suggest that the Hect domain E3 ubiquitin ligase Tom1 recruits Dia2 for degradation during G1 and G2/M phases of the cell cycle by recognizing specific, positively charged residues just upstream of the F-box domain. Failure to efficiently degrade Dia2 leads to defects in cell cycle dynamics.

Our data suggest that the proteolytic inhibition of Dia2 degradation that occurs as cells enter S phase or activate the S-phase

arrest was monitored by flow cytometry. (C) Dia2 is stabilized in *tom1*Δ and *tom1C3235A* mutants in G2/M phase. Wild-type, *tom1*Δ and *tom1C3235A* cells were arrested with nocodazole (15 μg/ml) for 3 h. Stability assays were performed as in (A and B). The results of quantification of Dia2 turnover in wild-type, *tom1*Δ and *tom1C3235A* strains are shown in the graph. Error bars indicate standard deviations. Flow cytometry was used to examine the nocodazole arrest. (D) Dia2 binding to Tom1 is regulated during the cell cycle. $Dia2^{MYC}$ and $Tom1^{FLAG}$ $Dia2^{MYC}$ cells were arrested with αF, HU, and nocodazole for 3 h, as in (A–C), respectively. Total cell lysates (2 mg) of the indicated strains were immunoprecipitated with anti-Flag antibodies and immunoblotted with anti-Flag and anti-Myc antibodies. The ratio of bound Dia2 to immunoprecipitated Tom1 was measured using Image J software. Flow cytometry was conducted to monitor the arrests in G1, S, and G2/M.

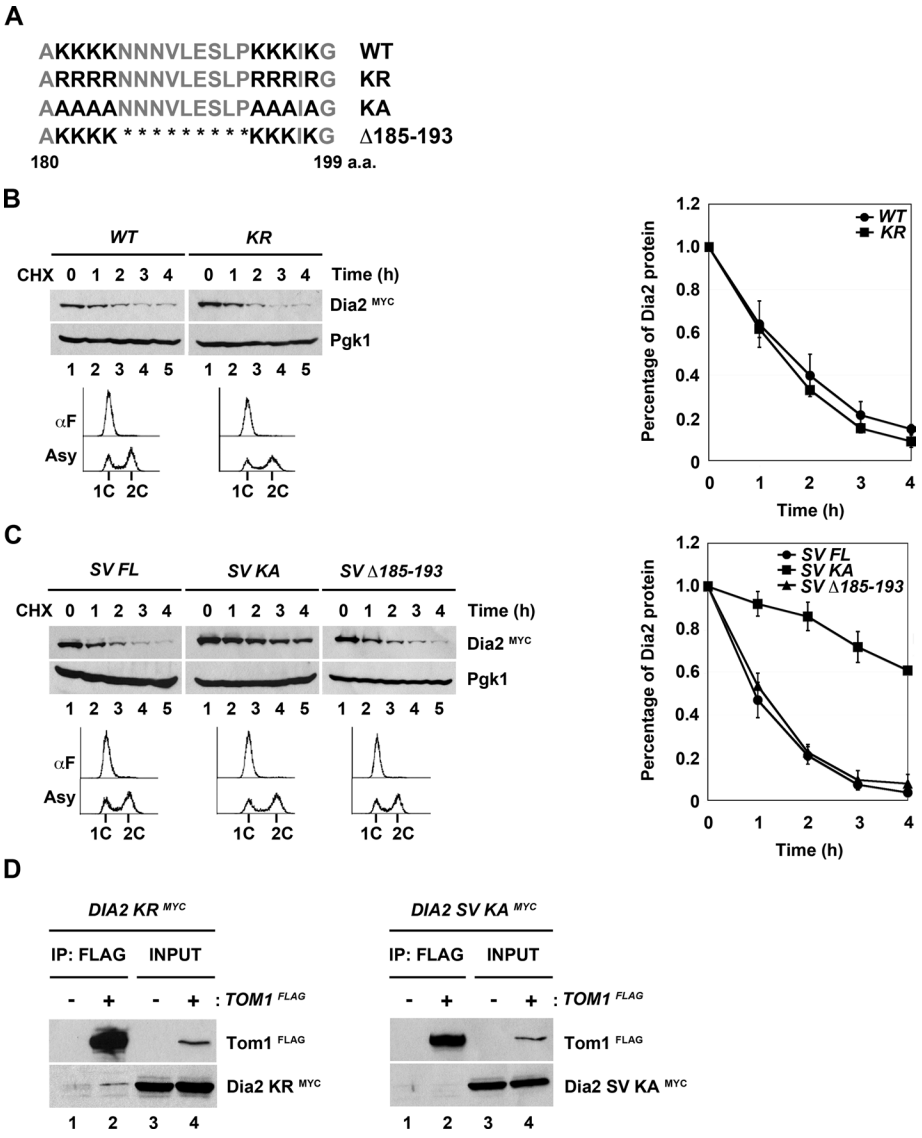

FIGURE 5: Tom1-mediated Dia2 proteolysis requires positively charged residues in the degradation domain of Dia2. (A) Domain containing the degradation/NLS region of Dia2. (B) Substitution of lysine for arginine does not stabilize Dia2 in G1. Wild-type and *dia2-KR* strains were arrested with αF for 3 h. Samples were taken at the indicated times and prepared for stability assay, as described in Figure 3A. Three independent results were used for quantification. Error bars indicate SDs. (C) The SVDia2-KA mutant protein is stabilized in G1 phase. The indicated strains were arrested with αF for 3 h. Stability assay was performed as in Figures 3A and 5B. SV, SV40 Tag NLS; FL, full-length Dia2. Quantification shows the rates of Dia2 turnover in the indicated strains. Error bars indicate SDs. (D) The SVDia2-KA mutant protein does not bind to Tom1. The indicated strains were grown to mid–log phase and used for a coimmunoprecipitation assay. Flag-tagged Tom1 was immunoprecipitated with anti-Flag antibodies. Immunoblot assay was conducted with anti-Flag and anti-Myc antibodies. See also Figure 4.

checkpoint depends on reduced binding between Dia2 and Tom1. In principle, such an outcome could be the result of a conformational change in Dia2, such as those that accompany posttranslational modifications, although there is currently no evidence for S phase–specific modification of Dia2. Alternatively, Tom1 has additional substrates and interaction partners that may compete for binding to Tom1 more effectively during S phase or in response to activation of the S-phase checkpoint. Interestingly, Tom1 targets excess histones for degradation when they are phosphorylated by the S-phase checkpoint kinase Rad53. Moreover, Tom1 physically interacts with Rad53 (Singh *et al.*, 2009), suggesting that it is possible that this role of Tom1 might influence its behavior during checkpoint activation. Future studies will be necessary to distinguish between these possibilities.

How Tom1 binds and recruits target proteins is an open question. Our results suggest that a short stretch of positively charged amino acids in Dia2 are required to bind Tom1. This domain may serve as a degron for targeting substrates to Tom1. The two other known targets of Tom1 include histone H3 (Singh *et al.*, 2009) and Yra1, an mRNA export factor (Iglesias *et al.*, 2010). Both proteins contain short stretches of positively charged amino acids, although neither shows a similarly spaced arrangement of residues, with the intervening sequence, as observed in Dia2 (unpublished data). It is possible that a single stretch of three to four positively charged residues on either side of the intervening sequence is sufficient for interaction with Tom1 or that the spacing of the positive charges does not play a role in recognition. Indeed, deletion of the intervening sequence does not alter Dia2 degradation kinetics, consistent with the idea that spacing of the residues does not play a role in recognition. We look forward to future studies investigating whether the motif we have identified serves as a recognition domain for other Tom1 targets.

Our previous work suggested a role for Dia2 degradation in cell cycle dynamics (Kile and Koepp, 2010). The results presented here confirm and extend those observations, showing that impaired degradation of Dia2 leads to a delay of the G1–to–S phase transition. However, the mechanism by which accumulated Dia2 slows the G1–to–S phase transition is not clear. One explanation might be that Dia2 has an as-yet-unidentified ubiquitination target that promotes G1 progression or S-phase entry. In this scenario, excess Dia2 would lead to inappropriate degradation of this unknown target. Alternatively, excess Dia2 may simply lead to a change in the balance of various SCF complexes by competing for core component proteins. For example, the relative concentration of those SCF complexes that have G1 ubiquitination substrates, such as SCF^{Cdc4}, which targets the Cdk inhibitor Sic1 and the DNA replication protein Cdc6 (Drury *et al.*, 1997; Skowyra *et al.*, 1997; Verma *et al.*, 1997), may be reduced. Regardless of the mechanism, these observations suggest that Dia2 protein levels are modulated throughout the cell cycle to prevent adverse effects on cell cycle progression.

In summary, we have identified a novel degradation pathway for the F-box protein Dia2 involving the Hect domain E3 ligase Tom1. Our work establishes a mechanistic basis for recognition of Dia2 by Tom1 and demonstrates a role for Dia2 degradation in cell cycle dynamics.

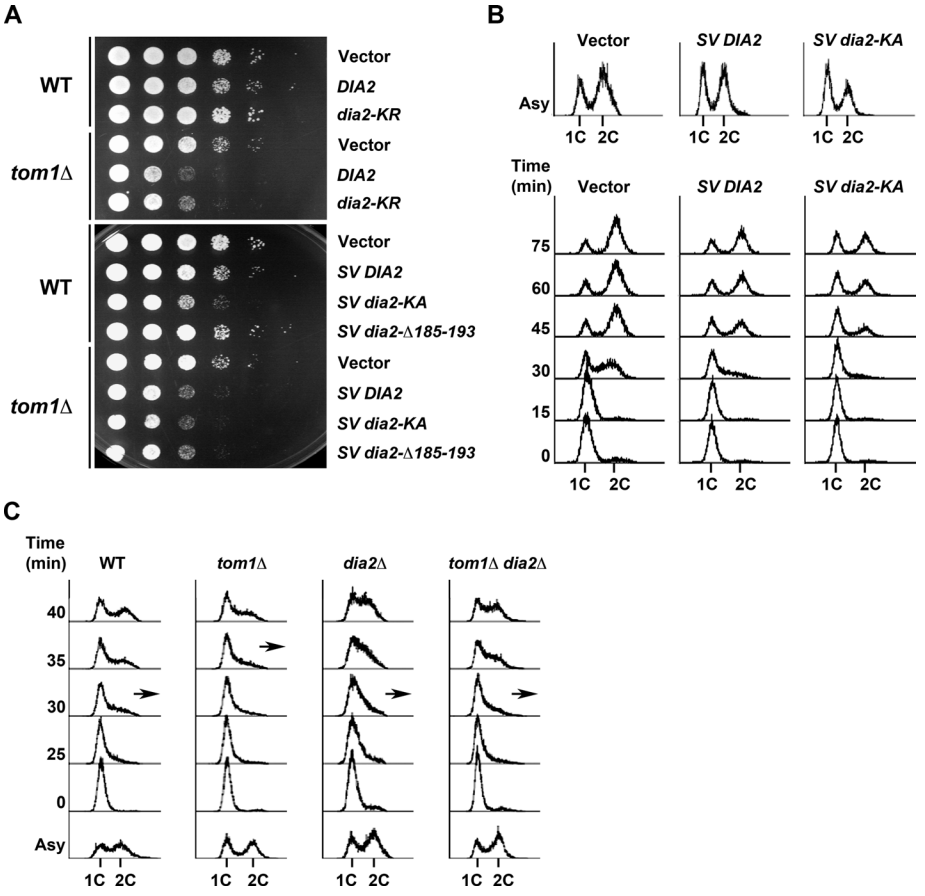

FIGURE 6: Tom1-mediated Dia2 turnover is required for efficient G1–to–S phase progression. (A) Overexpression of the *SVdia2-KA* mutant leads to a growth defect in wild-type cells. Wild-type and *tom1*Δ strains carrying the indicated galactose-inducible vectors were spotted in 10-fold dilutions onto minimal media containing 2% galactose. Plates were incubated at 30°C for 2–3 d. SV, SV40 Tag NLS. (B) Overexpression of the *SVdia2-KA* mutant causes a delay in G1–to–S phase progression. Wild-type cells carrying the indicated galactose-inducible plasmids were grown to mid–log phase in minimal media containing 2% galactose. Samples were processed for flow cytometry. Separately, cells were also arrested with αF for 3 h and released into minimal media containing 2% galactose and 15 μg/ml nocodazole. Samples were taken at the indicated times and prepared for flow cytometry. (C) Suppression of G1–to–S phase progression delay of *tom1*Δ mutant by deletion of *DIA2*. Wild-type, *tom1*Δ, *dia2*Δ, and *tom1*Δ *dia2*Δ cells were arrested with αF for 3 h and released into rich medium containing 15 μg/ml nocodazole. Samples taken at the indicated times were processed for flow cytometry. Arrows indicate start of S phase.

MATERIALS AND METHODS

Plasmids and strains

Yeast strains, plasmids, and oligonucleotides are described in Tables 1, 2, and 3. To generate the *tom1*Δ strain (DKY526), we replaced the open reading frame of *TOM1* with *KanMX* via homologous recombination in strain DKY153. The *TOM1-3FLAG* strain (DKY538) was generated using a previously described method (Gelbart *et al.*, 2001). The centromeric *9MYC-DIA2 KR*, *9MYC-SV40-DIA2-KA*, and *9MYC-SV40-Δ185-193* plasmids using a *GAL1,10* promoter (pDHK9, 10, and 11, respectively) were constructed via the generation of the KR or KA substitution and the deletion of the 185–193 fragment (Δ185-193) by the PCR stitching method, using the plasmids pACK135 or pACK176 with primers DHK107/108/109/110 and DHK112/113/114/115/116/117; this was followed by the amplification of the *KR*, *KA*, and *Δ185-193* fragments with primers DHK106 and 111. These fragments were then inserted into the *Mlu*I and *Hpa*I sites of the pACK135 or pACK176 plasmids. For construction of the 9MYC-*KR*, 9MYC-*SV40-KA*, and 9MYC-*SV40-Δ185-193* strains (DKY952, 968, and 969), the 9MYC-*KR*, 9MYC-*SV40-KA*, and 9MYC-*SV40-Δ185-193* fragments were cloned into the plasmids pACK142 and pACK181 with *Mlu*I and *Hpa*I sites to generate plasmids (pDHK12, 13, and 14, respectively). The plasmids (pDHK12, pDHK13, and pDHK14) linearized with the *Bcl*I restriction enzyme were integrated into strain DKY194 via homologous recombination.

Reverse transcription PCR (RT-PCR)

Cultures were grown to mid–log phase (2×10^7 cells/ml) at 30°C, and total RNA was isolated with PureLink Micro-to-Midi kit (Invitrogen, Carlsbad, CA), using the

Strain	Genotype	Source
DKY153	*ade2-1 ura3-1 leu2-3112 his3-11,15 trp1-1 can1-100 MAT a*	This study
DKY194	*dia2Δ::kanMX ade2-1 ura3-1 leu2-3112 his3-11,15 trp1-1 can1-100 MAT a*	This study
DKY526	*tom1Δ::kanMX ade2-1 ura3-1 leu2-3112 his3-11,15 trp1-1 can1-100 MAT a*	This study
DKY527	*tom1Δ::kanMX dia2Δ::kanMX ade2-1 ura3-1 leu2-3112 his3-11,15 trp1-1 can1-100 MAT a*	This study
DKY534	*tom1C3235A::URA3 ade2-1 ura3-1 leu2-3112 his3-11,15 trp1-1 can1-100 MAT a*	This study
DKY536	*tom1C3235A::URA3 dia2Δ::kanMX ade2-1 ura3-1 leu2-3112 his3-11,15 trp1-1 can1-100 MAT a*	This study
AKY149	*9MYC-DIA2::URA3 dia2Δ::kanMX ade2-1 ura3-1 leu2-3112 his3-11,15 trp1-1 can1-100 MAT a*	Kile and Koepp, 2010
DKY538	*TOM1-3XFLAG::kanMX ade2-1 ura3-1 leu2-3112 his3-11,15 trp1-1 can1-100 MAT a*	This study
DKY533	*tom1Δ::kanMX 9MYC-DIA2::URA3 dia2Δ::kanMX ade2-1 ura3-1 leu2-3112 his3-11,15 trp1-1 can1-100 MAT a*	This study
DKY558	*tom1C3235A::URA3 9MYC-DIA2::URA3 dia2Δ::kanMX ade2-1 ura3-1 leu2-3112 his3-11,15 trp1-1 can1-100 MAT a*	This study

TABLE 1: Yeast strains.

Continues

Strain	Genotype	Source
DKY540	*TOM1-3XFLAG::kanMX 9MYC-DIA2::URA3 dia2Δ::kanMX ade2-1 ura3-1 leu2-3112 his3-11,15 trp1-1 can1-100 MAT a*	This study
AKY192	*9MYC-dia2-TPR::URA3 dia2Δ::kanMX ade2-1 ura3-1 leu2-3112 his3-11,15 trp1-1 can1-100 MAT a*	Kile and Koepp, 2010
DKY596	*TOM1-3XFLAG::kanMX 9MYC-dia2-TPR::URA3 dia2Δ::kanMX ade2-1 ura3-1 leu2-3112 his3-11,15 trp1-1 can1-100 MAT a*	This study
AKY188	*9MYC-dia2-ΔF::URA3 dia2Δ::kanMX ade2-1 ura3-1 leu2-3112 his3-11,15 trp1-1 can1-100 MAT a*	Kile and Koepp, 2010
DKY904	*TOM1-3XFLAG 9MYC-dia2-ΔF::URA3 dia2Δ::kanMX ade2-1 ura3-1 leu2-3112 his3-11,15 trp1-1 can1-100 MAT a*	This study
AKY199	*9MYC-dia2-ΔN149::URA3 dia2Δ::kanMX ade2-1 ura3-1 leu2-3112 his3-11,15 trp1-1 can1-100 MAT a*	Kile and Koepp, 2010
DKY592	*TOM1-3XFLAG 9MYC-dia2-ΔN149::URA3 dia2Δ::kanMX ade2-1 ura3-1 leu2-3112 his3-11,15 trp1-1 can1-100 MAT a*	This study
AKY240	*9MYC-SV40NLS-dia2-ΔNLS::URA3 dia2Δ::kanMX ade2-1 ura3-1 leu2-3112 his3-11,15 trp1-1 can1-100 MAT a*	Kile and Koepp, 2010
DKY595	*TOM1-3XFLAG 9MYC-SV40NLS-dia2-ΔNLS::URA3 dia2Δ::kanMX ade2-1 ura3-1 leu2-3112 his3-11,15 trp1-1 can1-100 MAT a*	This study
DKY952	*9MYC-dia2-KR::URA3 dia2Δ::kanMX ade2-1 ura3-1 leu2-3112 his3-11,15 trp1-1 can1-100 MAT a*	This study
DKY976	*TOM1-3XFLAG::kanMX 9MYC-dia2-KR::URA3 dia2Δ::kanMX ade2-1 ura3-1 leu2-3112 his3-11,15 trp1-1 can1-100 MAT a*	This study
AKY238	*9MYC-SV40NLS-DIA2::URA3 dia2Δ::kanMX ade2-1 ura3-1 leu2-3112 his3-11,15 trp1-1 can1-100 MAT a*	Kile and Koepp, 2010
DKY968	*9MYC-SV40NLS-dia2-KA::URA3 dia2Δ::kanMX ade2-1 ura3-1 leu2-3112 his3-11,15 trp1-1 can1-100 MAT a*	This study
DKY979	*TOM1-3XFLAG::kanMX 9MYC-SV40NLS-dia2-KA::URA3 dia2Δ::kanMX ade2-1 ura3-1 leu2-3112 his3-11,15 trp1-1 can1-100 MAT a*	This study
DKY969	*9MYC-SV40NLS-dia2-Δ185-193::URA3 dia2Δ::kanMX ade2-1 ura3-1 leu2-3112 his3-11,15 trp1-1 can1-100 MAT a*	This study

TABLE 1: Yeast strains. Continued

manufacturer's protocol. After DNase I treatment, 3 μg total RNA was reverse transcribed using Superscript II (Invitrogen) with oligo $(dT)_{50}$ primer. The cDNA was amplified with primers DHK16 and 17 or ACT1-5 and ACT1-3.

In vitro binding assays

One milligram of total cell lysate isolated from baculovirus-infected Hi5 insect cells was immunoprecipitated with anti-Flag M2 monoclonal (Sigma-Aldrich, St. Louis, MO) or anti-Myc 9E10 monoclonal (Covance, Princeton, NJ) antibodies and immunoblotted with anti-Flag M2 and anti-Myc 9E10 antibodies.

Stability assays

Cells at 2×10^7 cells/ml were arrested with 40 μg/ml αF, 200 mM HU, or 15 μg/ml nocodazole for 3 h. Cycloheximide was added at 100 μg/ml. Cell pellets were washed and lysed by vortexing with glass beads in 20% trichloroacetic acid for 3 min (Kile and Koepp, 2010). Lysed cell pellets were centrifuged at 3000 rpm for 10 min and resuspended in Laemmli buffer. Precipitated proteins were neutralized with 1M Tris and boiled for 5 min. Protein concentration was quantified using the RC/DC protein assay kit (Bio-Rad, Hercules, CA). Proteins (20 μg) were run on 8% SDS–PAGE. Protein abundance was measured using the Image J software and normalized against a loading control.

Plasmid	Features	Source
p1219	*GAL1,10* promoter, *CEN TRP1 Amp^r*	Liu *et al.*, 1998
pACK135	*GAL1,10* promoter, *9MYC-DIA2 CEN TRP1 Amp^r*	Kile and Koepp, 2010
pACK176	*GAL1,10* promoter, *9MYC-SV40NLS-DIA2 CEN TRP1 Amp^r*	Kile and Koepp, 2010
pDHK9	*GAL1,10* promoter, *9MYC-dia2-KR CEN TRP1 Amp^r*	This study
pDHK10	*GAL1,10* promoter, *9MYC-SV40NLS-dia2-KA CEN TRP1 Amp^r*	This study
pDHK11	*GAL1,10* promoter, *9MYC-SV40NLS-dia2-Δ185-193 CEN TRP1 Amp^r*	This study
pDHK12	pRS406 1-kb *5′DIA2 UTR 9 9MYC-dia2-KR URA3 Amp^r*	This study
pDHK13	pRS406 1-kb *5′DIA2 UTR 9 9MYC-SV40NLS-dia2-KA URA3 Amp^r*	This study
pDHK14	pRS406 1-kb *5′DIA2 UTR 9 9MYC-SV40NLS-dia2-Δ185-193 URA3 Amp^r*	This study

TABLE 2: Plasmids used in this study.

Oligonucleotide	Sequence (5′–3′)
DHK3	GTTCACTATTATTGGCAATCAATGAAGGGCATGAAGGGTTTGGTCTTGCCAGGGAACAAAAGCTGGAGCTC
DHK4	CGTTCTAAAATACTTGGTTACATGGCGCTATAAATTTACACGAAAAATGACTATAGGGCGAATTGGGTACC
DHK16	GGGAATAGTAGAAGAAAAGG
DHK17	CAATTGGATATAGCTTGTTC
ACT1-5	ACAACGAATTGAGAGTTGCCCCAG
ACT1-3	AATGGCGTGAGGTAGAGAGAAACC
DHK106	GGAATTCCATATGTCTTCCCCAGGGAATTC
DHK107	GAGGAGACCAAAATAGCAAGAAGAAGAAGGAATAATAATGTTCTAGAA
DHK108	TTCTAGAACATTATTATTCCTTCTTCTTCTTGCTATTTTGGTCTCCTC
DHK109	TCGTTACCAAGGAGGAGGATTAGAGGTAGTACC
DHK110	GGTACTACCTCTAATCCTCCTCCTTGGTAACGA
DHK111	GCAGAACCACTTATCGATGTCCCCATTAGATCCAAC
DHK112	GAGGAGACCAAAATAGCAGCAGCAGCAGCGAATAATAATGTTCTAGAA
DHK113	TTCTAGAACATTATTATTCGCTGCTGCTGCTGCTATTTTGGTCTCCTC
DHK114	TCGTTACCAGCGGCGGCGATTGCAGGTAGTACC
DHK115	GGTACTACCTGCAATCGCCGCCGCTGGTAACGA
DHK116	GAGGAGACCAAAATAGCAAAAAAAAAAAAAGAAGAAGAAGATTAAAGGTAGTACCAAGAAA
DHK117	TTTCTTGGTACTACCTTTAATCTTCTTCTTCTTTTTTTTTTTTTGCTATTTTGGTCTCCTC

TABLE 3: Oligonucleotides used in this study.

Immunoprecipitation

Cells were cultured to mid–log phase (2×10^7 cells/ml) and collected by centrifuging at 4000 rpm for 2 min. Total cell lysate was isolated by vortexing the cells with glass beads in 0.3% CHAPS buffer (0.3% CHAPS, 40 mM HEPES, pH 7.4, 120 mM NaCl, 1 mM EDTA, 50 mM NaF, 10 mM glycerol 2-β) with protease inhibitor cocktail (Roche, Indianapolis, IN) for 40 min at 4°C. Protein concentration was determined using the Bio-Rad protein assay (Bio-Rad). Total lysate (2 mg) was incubated with anti-Flag M2 monoclonal (Sigma-Aldrich) antibodies and protein A/G agarose (Santa Cruz Biotechnology, Santa Cruz, CA) for 3 h at 4°C. Samples were washed with CHAPS buffer 4 times and boiled in Laemmli buffer for 5 min.

In vitro ubiquitination assays

Fractionated yeast extracts (50 µg) were incubated with 50 µg ubiquitin, 50 nM E1, 10 mM ATP, 60 mM creatine phosphate, 1 mM magnesium acetate, 150 µg/ml creatine kinase, and 40 µg GST-Dia2 protein bound to the glutathione-Sepharose 4B beads (GE Healthcare, Waukesha, WI) at 30°C for 45 min. Samples were run on 6% SDS–PAGE and immunoblotted with anti-GST polyclonal antibodies (Santa Cruz Biotechnology).

ACKNOWLEDGMENTS

This work was supported by a National Institutes of Health grant (R01 GM076663) to D.M.K. We thank C. Brandl (University of Western Ontario) for the gift of *tom1C3235A* strain.

REFERENCES

Blake D, Luke B, Kanellis P, Jorgensen P, Goh T, Penfold S, Breitkreutz BJ, Durocher D, Peter M, Tyers M (2006). The F-box protein Dia2 overcomes replication impedance to promote genome stability in *Saccharomyces cerevisiae*. Genetics 174, 1709–1727.

Drury LS, Perkins G, Diffley JF (1997). The Cdc4/34/53 pathway targets Cdc6p for proteolysis in budding yeast. EMBO J 16, 5966–5976.

Gelbart ME, Rechsteiner T, Richmond TJ, Tsukiyama T (2001). Interactions of Isw2 chromatin remodeling complex with nucleosomal arrays: analyses using recombinant yeast histones and immobilized templates. Mol Cell Biol 21, 2098–2106.

Iglesias N, Tutucci E, Gwizdek C, Vinciguerra P, Von Dach E, Corbett AH, Dargemont C, Stutz F (2010). Ubiquitin-mediated mRNP dynamics and surveillance prior to budding yeast mRNA export. Genes Dev 24, 1927–1938.

Kile AC, Koepp DM (2010). Activation of the S-phase checkpoint inhibits degradation of the F-box protein Dia2. Mol Cell Biol 30, 160–171.

Koepp DM, Kile AC, Swaminathan S, Rodriguez-Rivera V (2006). The F-box protein Dia2 regulates DNA replication. Mol Biol Cell 17, 1540–1548.

Kouranti I, Peyroche A (2012). Protein degradation in DNA damage response. Semin Cell Dev Biol 23, 538–545.

Kus BM, Caldon CE, Andorn-Broza R, Edwards AM (2004). Functional interaction of 13 yeast SCF complexes with a set of yeast E2 enzymes in vitro. Proteins 54, 455–467.

Liu Q, Li MZ, Leibham D, Cortez D, Elledge SJ (1998). The univector plasmid-fusion system, a method for rapid construction of recombinant DNA without restriction enzymes. Curr Biol 8, 1300–1309.

Mimura S, Komata M, Kishi T, Shirahige K, Kamura T (2009). SCF(Dia2) regulates DNA replication forks during S-phase in budding yeast. EMBO J 28, 3693–3705.

Morohashi H, Maculins T, Labib K (2009). The amino-terminal TPR domain of Dia2 tethers SCF(Dia2) to the replisome progression complex. Curr Biol 19, 1943–1949.

Nakayama KI, Nakayama K (2006). Ubiquitin ligases: cell-cycle control and cancer. Nat Rev Cancer 6, 369–381.

Pan X, Ye P, Yuan DS, Wang X, Bader JS, Boeke JD (2006). A DNA integrity network in the yeast *Saccharomyces cerevisiae*. Cell 124, 1069–1081.

Silverman JS, Skaar JR, Pagano M (2012). SCF ubiquitin ligases in the maintenance of genome stability. Trends Biochem Sci 37, 66–73.

Singh RK, Kabbaj MH, Paik J, Gunjan A (2009). Histone levels are regulated by phosphorylation and ubiquitylation-dependent proteolysis. Nat Cell Biol 11, 925–933.

Skowyra D, Craig KL, Tyers M, Elledge SJ, Harper JW (1997). F-box proteins are receptors that recruit phosphorylated substrates to the SCF ubiquitin-ligase complex. Cell 91, 209–219.

Swaminathan S, Kile AC, MacDonald EM, Koepp DM (2007). Yra1 is required for S phase entry and affects Dia2 binding to replication origins. Mol Cell Biol 27, 4674–4684.

Verma R, Feldman RM, Deshaies RJ (1997). SIC1 is ubiquitinated in vitro by a pathway that requires CDC4, CDC34, and cyclin/CDK activities. Mol Biol Cell 8, 1427–1437.

Zhou P, Howley PM (1998). Ubiquitination and degradation of the substrate recognition subunits of SCF ubiquitin-protein ligases. Mol Cell 2, 571–580.